2021 18th International Conference on Electrical Engineering, Computing Science and Automatic Control (CCE).
Mexico City, Mexico. November 10-12, 2021

Model Predictive Current Control of a Permanent Magnet Synchronous Machine with Exponential Cost Function

1st F. González Sáenz
ICBI - AACyE
UAEH
Hidalgo, Mexico
fbsaenz095@gmail.com

2nd O. Sandre Hernández
ICBI - AACyE
UAEH - CONACyT
Hidalgo, Mexico
omar_sandre@uaeh.edu.mx

***Abstract*—This paper presents the design of a continuous control set model predictive control (CCS-MPC) for a permanent magnet synchronous machine (PMSM). The CCS-MPC is designed for the control of the stator currents of a PMSM following a similar scheme to the one introduced in field-oriented control (FOC). In the presented CCS-MPC, the proposed cost function is modified by the introduction of a set of orthogonal functions known as Laguerre functions. Furthermore, an exponential cost function is introduced to afford long horizon predictions. The control law is derived by the formulation of a constrained optimization problem. By the introduction of the Laguerre functions and the exponential cost function, the computational burden is reduced and a long prediction horizon can be accomplished. Simulation results on Matlab/Simulink are presented to verify the performance of the proposed methodology.**

***Index Terms*—Model Predictive Current Control, Permanent Magnet Synchronous Machine, Exponential Cost Function**

I. Introduction

The permanent magnet synchronous machine (PMSM) has gained wide acceptance in moving control and transportation applications due to its high performance, high power density, low rotor inertia, high efficiency, and compact structure [1]. To achieve an accurate performance of the PMSM, high-performance control techniques are necessary such as field-oriented control (FOC), which allows performing a similar control to the one applied in DC motors [2]. The basic structure of FOC incorporates conventional PI controllers resulting in dynamic performance response limitations, this has motivate the development of different type of controllers for application in the PMSM such as sliding mode control [3], deadbeat control [4], fuzzy control [5], backstepping control [6], etc. Among all these control schemes, the development of predictive controllers depicts an alternative for robust control of the PMSM [7].

Model predictive control (MPC) has been widely implemented in the industry as an effective method to face control problems that include constraints, multi-variable control, and non-linearities [8], [9]. Two different control strategies regarding MPC can be found in the literature: Finite Control Set Model Predictive Control (FCS-MPC) [10], [11] and Continuous Control Set Model Predictive Control (CCS-MPC) [12], [13], both have been applied to electrical drivers. The FCS-MPC is based on the optimal voltage vector compute that minimizes a cost index preset, this MPC method yields a good transient state performance and provides a large control bandwidth. However, this method causes high torque and current ripples, especially in long sampling times. [14].

In the CCS-MPC method, the control algorithm is based on the prediction of the state variables according to a discrete model of the system. The predicted state variables are used in a cost function, which is evaluated over a prediction horizon to obtain the vector of future control actions. Unlike the FCS-MPC, a continuous duty cycle is obtained and applied through a PWM modulator such as space vector modulation (SVM). The advantages of this approach lie in an improvement of the total harmonic distortion (THD) of the three-phase currents, and in a fixed switching frequency [15].

A disadvantage of CCS-MPC is the high computational burden, which can result in system instability, due to matrices ill-conditioned, this is the main reason to restrict the prediction horizon to one step ahead in predictive control of PMSM. In [16], approximate dynamic programming is used to develop a computationally efficient direct model predictive current control. In [17], an integer least-squares problem for sphere decoding algorithm is proposed. An alternative to this approach is to use exponential cost function in the formulation of MPC as presented in [18]. This methodology can be extended to PMSM drives to perform MPC with long horizon predictions.

In this paper, the formulation of a CCS-MPC for the current control of a PMSM is proposed. The main contribution of the proposed methodology is the formulation of an exponential cost function, which is optimized for the selection of the control action. Thus, a computational burden reduction is obtained, preventing the numerical condition issue and hence, system instability. The speed loop is designed following a Lyapunov approach to provide robustness to load torque disturbances. The current loop is based on MPC and is designed based on the principle of receding horizon control taking into consideration the linearized PMSM discrete-time

978-1-6654-0029-9/21/$31.00 ©2021 IEEE

model. Simulations results in Matlab/Simulink are presented to validate the proposed methodology.

II. PMSM MATHEMATICAL MODEL

The PMSM dynamic can be modeled in the rotor reference frame $d-q$. The magnetic circuit is assumed to be linear (i.e. no saturation) with negligible iron losses, and the back EMF is assumed to be sinusoidal [2]. Furthermore, parametric variations are not considered. Thus, the voltage equations of the PMSM are given by:

$$\begin{aligned} u_{sd} &= R_s \cdot i_{sd} + L_{sd}\tfrac{d}{dt} i_{sd} - p\omega_m \cdot L_{sq} \cdot i_{sq}, \\ u_{sq} &= R_s \cdot i_{sq} + L_{sq}\tfrac{d}{dt} i_{sq} + p\omega_m \cdot (L_{sd} \cdot i_{sd} + \psi_{PM}), \end{aligned} \tag{1}$$

where L_{sd} and L_{sq} are the inductances in $d-q$ axis respectively; i_{sd} and i_{sq} are $d-q$ axis currents; ψ_{PM} is the permanent magnet flux of the rotor; R_s is the stator resistance for both $q-d$ axis; ω_m is the electrical speed; and u_{sd}, u_{sq} are the $d-q$ axis voltages. Since the PMSM under study is a surface PMSM, it is considered that $L_{sd} = L_{sq}$, and the following equation describes the electromagnetic torque M_e:

$$M_e = \frac{3}{2} p \left(\psi_{PM} \cdot i_{sq}\right), \tag{2}$$

where p is the pair of poles. The math model presented in (1) contains non-linear terms and coupled dynamics. A linear model of the PMSM can be obtained by decoupling the non-linear terms of (1) as in [19]. By defining the following variables:

$$\begin{aligned} u_{dd} &= u_d + p\omega_m \psi_q, \\ u_{qq} &= u_q - p\omega_m \psi_d, \end{aligned} \tag{3}$$

the state space model of a PMSM can be written as:

$$\frac{d\mathbf{x}(t)}{dt} = \mathbf{A_i}\mathbf{x}(t) + \mathbf{B_i}\mathbf{u}(t), \tag{4}$$

where

$$\mathbf{A_i} = \begin{bmatrix} -\frac{R_s}{L_s} & 0 \\ 0 & -\frac{R_s}{L_s} \end{bmatrix}, \quad \mathbf{B_i} = \begin{bmatrix} \frac{1}{L_s} & 0 \\ 0 & \frac{1}{L_s} \end{bmatrix}, \tag{5}$$

$$\mathbf{x(t)} = \begin{bmatrix} i_d \\ i_q \end{bmatrix}, \quad \mathbf{u}(t) = \begin{bmatrix} u_{dd} \\ u_{qq} \end{bmatrix}. \tag{6}$$

Conventionally, u_{sd} and u_{sq} are converted to PWM signals by the space vector modulation technique and are supplied to the PMSM by a power converter. Before this conversion, the system is decoupled, and the new control signals u_{dd}, and u_{qq} introduced in (3) are calculated for application in the power converter.

III. CCS-MPC DESIGN APPROACH

A. Predictions based on the Incremental model

MPC control is designed based on the mathematical model of the plant, commonly expressed as a state-space model. The continuous state-space model of the PMSM is converted in its equivalent discrete model based on the Euler forward discretization. This method is selected to keep a low computational burden, however, the small sampling time used preserves the stability of the discrete approximation. Furthermore, to reduce the error in steady-state, an incremental state-space model is used. The discrete state-space model can be written as [20]:

$$\begin{aligned} \begin{bmatrix} \Delta\mathbf{x}_m(k+1) \\ \mathbf{y}(k+1) \end{bmatrix} &= \begin{bmatrix} \mathbf{A}_m & \mathbf{o}_m^T \\ \mathbf{C}_m\mathbf{A}_m & \mathbf{I}_{q\times q} \end{bmatrix} \begin{bmatrix} \Delta\mathbf{x}_m(k) \\ \mathbf{y}(k) \end{bmatrix} \\ &\quad + \begin{bmatrix} \mathbf{B}_m \\ \mathbf{C}_m\mathbf{B}_m \end{bmatrix} \Delta\mathbf{u}(k), \end{aligned} \tag{7}$$

$$\mathbf{y}(k) = \begin{bmatrix} \mathbf{o}_m & \mathbf{I}_{q\times q} \end{bmatrix} \begin{bmatrix} \Delta\mathbf{x}_m(k) \\ \mathbf{y}(k) \end{bmatrix},$$

where $\Delta\mathbf{x}_m(k) = \mathbf{x}_m(k) - \mathbf{x}_m(k-1)$; $\Delta\mathbf{u}(k) = \mathbf{u}(k) - \mathbf{u}(k-1)$; $\mathbf{A}_m = \mathbf{I} + \mathbf{A}_i T_s$; $\mathbf{B}_m = \mathbf{B}_i T_s$; T_s is the sampling time; q is the number of outputs; and o_m is a zero matrix of appropriate dimensions. For notation simplicity, (7) is rewritten as:

$$\begin{aligned} \mathbf{x}(k+1) &= \mathbf{A}\mathbf{x}(k) + \mathbf{B}\Delta\mathbf{u}(k), \\ \mathbf{y}(k) &= \mathbf{C}\mathbf{x}(k). \end{aligned} \tag{8}$$

Based on the state-space model $(\mathbf{A}, \mathbf{B}, \mathbf{C})$, the prediction of the state variables from the sampling instant k_i over a finite prediction horizon N_P can be solved recursively from (8). The prediction of the state variables at $k_i + N_p$ can be obtained as follows:

$$\begin{aligned} \mathbf{x}(k_i + N_p \mid k_i) &= \mathbf{A}^{N_p}\mathbf{x}(ki) \\ &\quad + \sum_{i=0}^{N_c-1} \mathbf{A}^{N_p-i-1}\mathbf{B}\Delta\mathbf{u}(ki+i). \end{aligned} \tag{9}$$

Similarly, the predicted output over a control horizon N_c can be solved recursively based on the state prediction. The predicted output at $k_i + N_p$ can be obtained as follows:

$$\begin{aligned} \mathbf{y}(k_i + N_p \mid k_i) &= \mathbf{C}\mathbf{A}^{N_p}\mathbf{x}(ki) \\ &\quad + \sum_{i=0}^{N_c-1} \mathbf{C}\mathbf{A}^{N_p-i-1}\mathbf{B}\Delta\mathbf{u}(k_i+1). \end{aligned} \tag{10}$$

By defining the vectors $\mathbf{Y}$ and $\Delta\mathbf{U}$ as

$$\begin{aligned} \Delta\mathbf{U} &= \left[\Delta\mathbf{u}\left(k_i\right)^T \Delta\mathbf{u}\left(k_i+1\right)^T \ldots \Delta\mathbf{u}\left(k_i+N_c-1\right)^T\right]^T, \\ \mathbf{Y} &= \left[\mathbf{y}\left(k_i+1 \mid k_i\right)^T \mathbf{y}\left(k_i+2 \mid k_i\right)^T \ldots \mathbf{y}\left(k_i+N_p \mid k_i\right)^T\right]^T, \end{aligned} \tag{11}$$

The output $\mathbf{Y}$ can be written as:

$$\mathbf{Y} = \mathbf{F}\mathbf{x}\left(k_i\right) + \mathbf{\Phi}\Delta\mathbf{U}, \tag{12}$$

where

$$\mathbf{F} = \begin{bmatrix} \mathbf{CA} \\ \mathbf{CA}^2 \\ \mathbf{CA}^3 \\ \vdots \\ \mathbf{CA}^{N_p} \end{bmatrix}, \tag{13}$$

$$\mathbf{\Phi} = \begin{bmatrix} \mathbf{CB} & 0 & \dots & 0 \\ \mathbf{CAB} & \mathbf{CB} & \dots & 0 \\ \mathbf{CA}^2\mathbf{B} & \mathbf{CAB} & \dots & 0 \\ \vdots & & & \\ \mathbf{CA}^{N_p-1}\mathbf{B} & \mathbf{CA}^{N_p-2}\mathbf{B} & \dots & \mathbf{CA}^{N_p-N_c}\mathbf{B} \end{bmatrix}. \tag{14}$$

For a given set-point signal $r(k_i)$ at sample time k_i within a prediction horizon, the objective of the predictive control is to bring the predicted output as close as possible to the set-point signal. For simplicity, we assume that the set-point remains constant in the optimization window. This objective is then translated into a design to find the "best" control parameter vector $\Delta\mathbf{U}$ such that the error between the set-point and the predicted output is minimized.

B. Laguerre function approach

Due to complicated process dynamics and high demands on closed-loop performance, the solution of $\Delta\mathbf{U}$ may imply a heavy computational load. Instead, an alternative approach is to use Laguerre networks in the design of model predictive control [21].

The control trajectory can be determined by a set of Laguerre functions as:

$$\Delta u(k_i + k) = \sum_{j=1}^{N} c_j(k_i)\, l_j(k) = L(k)^T \eta, \tag{15}$$

where $L(k) = [l_1(k) l_2(k) \dots l_N(k)]^T$; $\eta = [c_1 c_2 \dots c_N]^T$; N is the number of terms used in the expansion; $c_j, j = 1, 2, \dots, N$, and $l_j(k)$ are the coefficients and the set of the Laguerre functions respectively. The Laguerre functions can be constructed recursively as [22]:

$$L(k+1) = A_l L(k), \tag{16}$$

where

$$A_l = \begin{bmatrix} a & 0 & 0 & \dots & 0 \\ \beta & a & 0 & \dots & 0 \\ -a\beta & \beta & a & \dots & 0 \\ \vdots & \vdots & \ddots & \ddots & \vdots \\ (-1)^{N-2}a^{N-2}\beta & (-1)^{N-3}a^{N-3}\beta & \dots & \beta & a \end{bmatrix},$$

$$L(0)^T = \sqrt{\beta}\begin{bmatrix} 1 & -a & a^2 & -a^3 & \dots & (-1)^{N-1}a^{N-1} \end{bmatrix},$$

where $\beta = 1 - a^2$; and $0 \le a < 1$ is the pole of the discrete Laguerre network. For a multiple-input multiple-output (MIMO) system, each control input $\Delta\mathbf{u}_m$ is associated to their respective set of Laguerre functions L_m and coefficients η_m respectively. Thus, by using (9) and (15) the prediction of the future state variable becomes:

$$\mathbf{x}(k_i + N_p \mid k_i) = \mathbf{A}^{N_p}\mathbf{x}(ki) + \sum_{i=0}^{N_p-1} \mathbf{A}^{N_p-i-1}\Big[\mathbf{B}_1 L_1(i) + \mathbf{B}_2 L_2(i) + \dots + \mathbf{B}_m L_m(i)\Big]\eta_p, \tag{17}$$

where $\eta_p^T = [\ \eta_1^T \quad \eta_2^T \quad \dots \quad \eta_m^T\ ]$; and $\mathbf{B}_1, \mathbf{B}_2, \dots, \mathbf{B}_m$ is the $i-$column of the $\mathbf{B}$ matrix in the incremental model. Thus, the variable to be optimized are the coefficients of the Laguerre functions.

C. Control Law

To determine the coefficients η_p of the Laguerre functions, the formulation of a constrained optimization problem is presented. Then, the control law is obtained by the minimization of the following exponential cost function J [18]:

$$\begin{aligned} J = &\sum_{j=1}^{N_p} \alpha^{-2j}\mathbf{x}(k_i + j \mid k_i)^T \mathbf{Q}_\alpha \mathbf{x}(k_i + j \mid k_i) \\ &+ \sum_{j=0}^{N_p} \alpha^{-2j}\Delta\mathbf{u}(k_i + j)^T \mathbf{R}_\alpha \Delta\mathbf{u}(k_i + j), \end{aligned} \tag{18}$$

subject to

$$\mathbf{u}_{min} \le M\eta + \mathbf{u}(k-1) \le \mathbf{u}_{max},$$

where

$$M = \begin{bmatrix} \sum_{i=0}^{k-1} L_1(i)^T & \mathbf{o}_2^T & \dots & \mathbf{o}_m^T \\ \mathbf{o}_1^T & \sum_{i=0}^{k-1} L_2(i)^T & \dots & \mathbf{o}_m^T \\ \vdots & \vdots & \vdots & \vdots \\ \mathbf{o}_1^T & \mathbf{o}_2^T & \dots & \sum_{i=0}^{k-1} L_m(i)^T \end{bmatrix},$$

$$\begin{aligned} \gamma &= \frac{1}{\alpha}, \\ \mathbf{Q}_\alpha &= \gamma^2\mathbf{Q} + \left(1 - \gamma^2\right)\mathbf{P}_\infty, \\ \mathbf{R}_\alpha &= \gamma^2\mathbf{R}, \end{aligned}$$

and P_∞ is the solution of the algebraic Riccati equation:

$$\mathbf{A}^T\Big[\mathbf{P}_\infty - \mathbf{P}_\infty\mathbf{B}\big(\mathbf{R} + \mathbf{B}^T\mathbf{P}_\infty\mathbf{B}\big)^{-1}\mathbf{B}^T\mathbf{P}_\infty\Big]\mathbf{A} + \mathbf{Q} - \mathbf{P}_\infty = 0.$$

In (18), $\alpha > 1$; $\mathbf{Q} \ge 0, \mathbf{R} > 0$ are given, and $\mathbf{Q}_\alpha \ge 0$, $\mathbf{R}_\alpha > 0$ are matrices of appropriate dimensions; $\mathbf{o}_k, k = 1, 2, ..., m$ is a zero row vector of $L(0)^T$ dimensions; u_{min}, u_{max} are the lower and upper limit in the control input. It can be seen in (18) that the state variables and the control input are associated with their respective exponential factor, therefore, the original system is transformed by the new variables

$$\begin{aligned} \Delta\hat{\mathbf{u}}(k+j) &= \alpha^{-j}\Delta\mathbf{u}(k_i + j), \\ \hat{\mathbf{x}}(k_i + j \mid k_i) &= \alpha^{-j}x(k_i + j \mid k_i), \end{aligned} \tag{19}$$

which lead (8) to the following system:

$$\hat{\mathbf{x}}(k_i + j + 1 \mid k_i) = \hat{\mathbf{A}}\hat{\mathbf{x}}(k_i + 1 \mid k_i) + \hat{\mathbf{B}}\Delta\hat{\mathbf{u}}(k_i). \tag{20}$$

where $\hat{\mathbf{A}} = \frac{A}{\alpha}$ and $\hat{\mathbf{B}} = \frac{B}{\alpha}$. By using these exponentially weighted variables, the exponentially weighted cost function is expressed in terms of the transformed variables, and the construction (13)-(14) is now based on the pair ($\alpha^{-1}\mathbf{A}$, $\alpha^{-1}\mathbf{B}$). The exponential feasibility is presented in [18]. Thus, the eigenvalues do not take a large value, avoiding the ill-conditioned matrix problem.

IV. Current Control of the PMSM

For simplicity, the control of the PMSM is commonly performed in a cascade control approach, an outer loop is used to regulate the speed of the machine and follow the reference speed, and an inner loop to regulate the $d-q$ stator currents and follow the reference current. In this section, the CCS-MPC presented in section III is developed for the current control of the PMSM. It is assumed that the $d-q$ currents are measurable and available for feedback. There are mainly two steps necessary in predictive control, the prediction of the output, and the derivation of the control law.

A. Output prediction

For the current control of the PMSM, the $d-q$ components of the stator current are selected as the state variables, and the $d-q$ components of the stator voltage as the control input. Then, by using $\hat{\mathbf{y}}(k) = \hat{\mathbf{x}}(k) = [\ i_d(k) - i_d(k-1) \quad i_q(k) - i_q(k-1) \quad i_d(k) \quad i_q(k)\ ]^T$, and $\mathbf{u}(k) = [\ u_d(k) \quad u_q(k)\ ]^T$, the output prediction can be obtained from (17) as:

$$\hat{\mathbf{y}}(k_i + N_p \mid k_i) = \hat{\mathbf{A}}^{N_p}\hat{\mathbf{x}}(ki) + \phi(m)^T\eta_p, \tag{21}$$

where

$$\phi(m) = \textstyle\sum_{i=0}^{N_p-1}\hat{\mathbf{A}}^{N_p-i-1}\left[\hat{\mathbf{B}}_1 L_1(i) + \hat{\mathbf{B}}_2 L_2(i)\right],$$
$$\eta_p^T = [\ \eta_1^T \quad \eta_2^T\ ].$$

note that each element of ϕ can be solved recursively independently, and for a linear time-invariant system it can be calculated offline for the evaluation in the cost function.

B. Cost function formulation

For regulation of the state variables, the cost function (18) can be used for a given $\mathbf{Q}_\alpha$ and $\mathbf{R}_\alpha$. In the case of reference tracking, the state variables are reformulated as the difference between the reference point and the output of the system. Thus, by defining the i_d^* and i_q^* as the $d-q$ reference currents respectively, the state variables are rewritten as $\hat{\mathbf{x}}(k) = [i_d(k) - i_d(k-1), i_q(k) - i_q(k-1), i_d(k) - i_d^*, i_q(k) - i_q^*]^T$. Thus, by using the predictive output given by (21), and the Laguerre functions for $\Delta\mathbf{u}$, the cost function can be written as:

$$J = \sum_{j=1}^{N_p} \hat{\mathbf{x}}\left(k_i + j \mid k_i\right)^T \mathbf{Q}_\alpha \hat{\mathbf{x}}\left(k_i + j \mid k_i\right) + \eta_p^T \mathbf{R}_\alpha \eta_p. \tag{22}$$

In (22), the $\mathbf{R}_\alpha$ and $\mathbf{Q}_\alpha$ matrices are used to balance the trade-off in the reference tracking and the control action. $\mathbf{Q}_\alpha$ can be selected as the identity matrix for an equal trade-off between the i_d and the i_q reference tracking. For $\mathbf{R}_\alpha$, a large value will tend to penalize the control action, leading to slow response in the current reference tracking. To find the optimal coefficients of the Laguerre functions η_p, the cost function J is minimized as a constrained optimization problem. In this way,

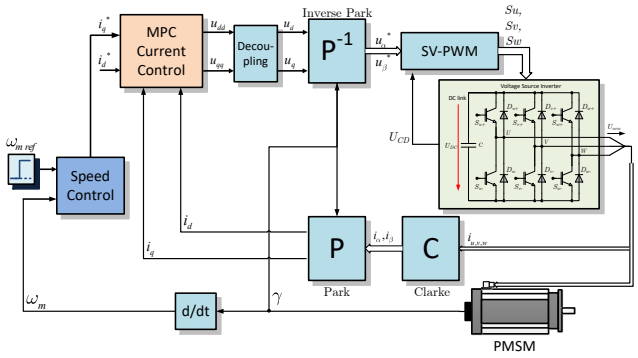

Fig. 1. Simplified block diagram of the proposed control scheme

TABLE I
PARAMETERS OF THE PMSM

282V, 3-Φ, PMSM			
Parameter	**value**	**Parameter**	**value**
M_{LN}	4.7 Nm	p	3
R_s	2.41 Ω	Ω_{nom}	3000 Rpm
L_{sd}	24 mH	L_{sq}	24 mH
ψ_{PM}	0.2456 Vs	i_N	3.4 A
J	$3.041 \cdot 10^{-}3 \quad kgm^2$		

by replacing (21) in (22), the optimization of the formulated cost function is rewritten as:

$$\begin{aligned} J = & min_{\eta_p} \quad \eta_p^T\mathbf{\Omega}\eta_p + 2\eta_p^T\mathbf{\Psi}\hat{\mathbf{x}}(k_i) + \mathbf{\Gamma}, \\ & s.t. \qquad \mathbf{u}_{min} \leq M\eta + \mathbf{u}(k-1) \leq \mathbf{u}_{max}. \end{aligned} \tag{23}$$

where

$$\mathbf{\Omega} = \textstyle\sum_{m=1}^{N_p}\phi(m)\mathbf{Q}_\alpha\phi(m)^T + \mathbf{R}_\alpha,$$
$$\mathbf{\Psi} = \textstyle\sum_{m=1}^{N_p}\phi(m)\mathbf{Q}_\alpha\hat{\mathbf{A}}^m,$$
$$\mathbf{\Gamma} = \textstyle\sum_{m=1}^{N_p}\hat{\mathbf{x}}(k_i)^T(\hat{\mathbf{A}}^T)^m\mathbf{Q}_\alpha\hat{\mathbf{A}}^m\hat{\mathbf{x}}(ki).$$

The solution of (23) is performed based on dynamic programming. In this paper, Hildreth's quadratic programming algorithm is used [23]. The solution of (23) will lead to the optimal control trajectory to follow the current reference, however, by the principle of receding horizon control, only the first element of the optimal trajectory is applied to the PMSM. Therefore, the control $(u_d(k), u_q(k))$ can be determined as:

$$\mathbf{u}(k) = \mathbf{u}(k-1) + \begin{bmatrix} L_1(0)^T & \mathbf{o}_2^T \\ \mathbf{o}_1^T & L_2(0)^T \end{bmatrix}\eta_p. \tag{24}$$

V. Simulation Results

A simplified block diagram of the proposed methodology is presented in Fig. 1. The proposed control scheme is based on the structure of conventional FOC. Since the dynamic response of the mechanical speed is slower than the dynamic response of the $d-q$ currents, the speed control can be used to set the reference of the i_q current for the CCS-MPC, while the reference of the i_d current is set to zero to obtain a constant torque angle control. The speed control used is based on the control presented in [24], which is discretized based on Euler

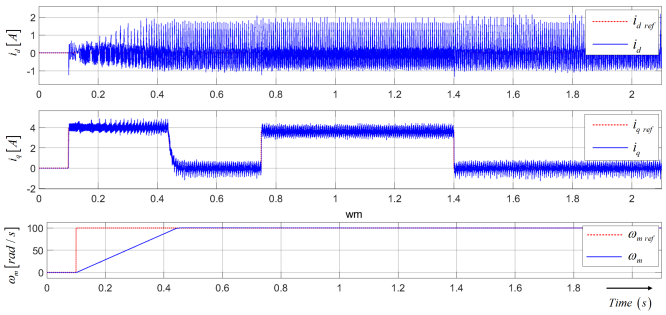

Fig. 2. Closed-loop system response without exponential weighting. From top: i_d current, i_q current, mechanical speed.

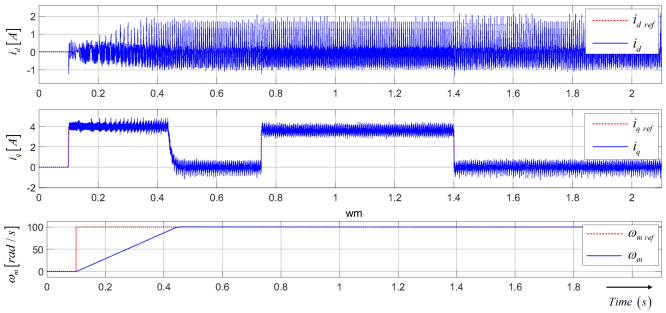

Fig. 3. Closed-loop system response with exponential weighting. From top: i_d current, i_q current, mechanical speed.

differentiation. Finally, the reference voltage vector is applied to the PMSM through the space vector pulse width modulation (SV-PWM).

To verify the performance of the proposed control methodology, the block diagram shown in Fig. 1 has been implemented in Matlab/Simulink. The parameters of the PMSM under test are listed in Table I. A comparison between the simulation of the unweighted control scheme and the exponentially weighted control scheme under steady and transient operation is presented. For both control schemes, a sampling time of $60\mu s$ is used, and the parameters used in the CCS-MPC were adjusted by several simulations. The final values of the parameters used in this simulation are the following: $N_p = 150$, $N_c = 10$, $\mathbf{Q} = \mathbf{C}\mathbf{C}^T$, $\mathbf{R} = 0.01$, $a = 0.8$, $N = 15$, $\alpha = 1.2$ and u_{min}, u_{max} are calculated to keep the reference voltage vector applied by the SVM-PWM in the linear region.

The performance under steady-state evaluation with and without exponential cost function is shown in Figs. 2-3 respectively. The speed reference is set at 100 rad/s. At the time instant of $0.7s$ a torque load disturbance of $4Nm$ is applied to the machine and is maintained for $0.7s$ until is released at a time of $1.4s$. The results showed a fast dynamic response of the i_d and i_q currents, and accurate tracking of the reference speed. When the disturbance is applied to the machine, the control can mitigate the load torque and remain stable during the time the disturbance is applied. It can be seen in the results, that the application of the control voltage through the PWM leads to some noise in the current performance, this ripple can be reduced by using an smaller sampling time. It is possible to

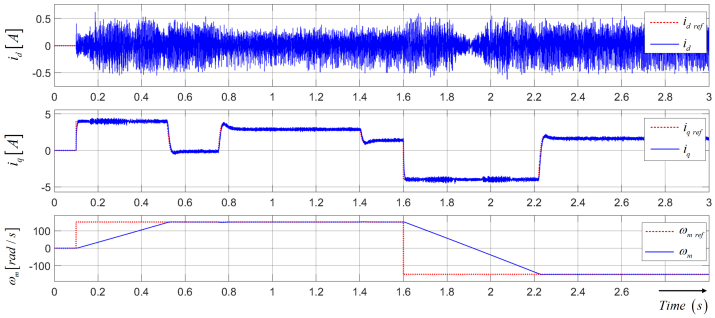

Fig. 4. Response under reversal speed of the PMSM without exponential weighting. From top: i_d current, i_q current, mechanical speed

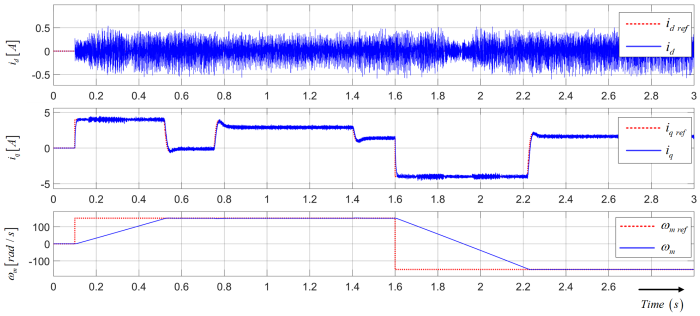

Fig. 5. Response under reversal speed of the PMSM with exponential weighting. From top: i_d current, i_q current, mechanical speed

TABLE II
EIGENVALUES AND CONDITION NUMBER FOR BOTH WEIGHTED AND UNWEIGHTED SYSTEMS

Eigenvalues				
N_p	Unweighted		Weighted	
	$\lambda_{min}(\Omega)$	$\lambda_{max}(\Omega)$	$lambda_{min}\Omega$	$\lambda_{max}\Omega$
10	6×10^{-4}	0.0071	4.1667×10^{-4}	0.0038
30	6×10^{-4}	0.4173	4.1667×10^{-4}	0.0116
300	6.0066×10^{-4}	1.3092×10^{3}	4.3829×10^{-4}	0.0165
Condition Number $\mathcal{K}(\Omega)$				
10	12.7968		9.0077	
30	695.5065		27.7608	
300	2.1796 $\times10^{6}$		37.6127	

observe in both control schemes that the performance is similar because the optimal solution of the exponentially weighted cost function is equivalent to the original solution.

The performance of the proposed control scheme under the dynamic state is shown in Figs. 4-5 respectively. In this test, the evaluation of the PMSM under speed reversal is performed. At time $t = 0.1s$ the reference is set to 150 rad/s and after $1.5s$ the speed reference is changed to -150 rad/s. Figs. 4-5 shown a fast dynamic response of the currents, and an accurate speed reference tracking. Similar to the results under steady-state, the disturbance load torque is mitigated by the control.

To evaluate the effect of the computational burden of the CCS-MPC under long horizon predictions, the condition number $\mathcal{K}(\mathbf{\Omega})$ and the eigenvalues of $\mathbf{\Omega}$ are calculated. In this evaluation, the prediction horizon is evaluated for $N_p = 10, 30, 300$, and the results are shown in Table II for the condition number and the eigenvalues respectively. It

is observed that the condition number $\mathcal{K}(\mathbf{\Omega})$ is significantly reduced for long horizon predictions, this is mainly because the optimization problem is performed using the exponential cost function. In the same way, with the modification of the original cost function, the Ω eigenvalues are significantly reduced for long horizon predictions. By doing so, a long prediction horizon can be used safely.

The results obtained demonstrate the effectiveness of the proposed control scheme, which can successfully control the speed and current of a PMSM despite torque load disturbances. With the application of the proposed exponential cost function, the CCS-MPC can be performed for long-horizon predictions, leading to robust control of the PMSM. Moreover, the numerical ill-condition of long-horizon CCS-MPC is significantly reduced by the exponential factor used in the cost function. A drawback of the proposed methodology is the number of parameters required to operate accurately in the PMSM control. These parameters have been adjusted on trial and error, and further research is necessary to determine the parameters of the proposed CCS-MPC. Furthermore, large parametric variations could lead to errors in the output prediction, and then in the control signal. Finally, in the real system, the processing time of the digital system should be less than the sampling time to guarantee a correct performance of the CCS-MPC.

VI. Conclusions

In this paper, an exponential cost function for the CCS-MPC of a PMSM is proposed. The CCS-MPC is formulated for the stator current control of the PMSM, and the application of the proposed methodology results in robust control of the PMSM under torque load disturbances. It can be observed from the simulations results, that the PMSM follows the reference under steady and dynamic operation.

The exponential cost function is formulated to reduce the computational burden of long-horizon predictions in CCS-MPC, this is verified by the calculation of the condition number and the eigenvalues of the matrix required for the state prediction. In the same way, the proposed exponential cost function reduces the numerical ill-condition in CCS-MPC. The obtained results demonstrate that the proposed methodology is an alternative to implement long horizon predictions in electrical drives. Further research can be oriented to the sensorless operation of the proposed scheme, this issue will be investigated in the future.

References

[1] R. Krishnan, *Permanent magnet synchronous and brushless DC motor drives*. CRC press, 2017.

[2] M. Wishart, G. Diana, and R. Harley, "Controller design for applying field-oriented control to the permanent magnet synchronous machine," *Electric power systems research*, vol. 19, no. 3, pp. 219–227, 1990.

[3] S. Li, M. Zhou, and X. Yu, "Design and implementation of terminal sliding mode control method for pmsm speed regulation system," *IEEE Transactions on Industrial Informatics*, vol. 9, no. 4, pp. 1879–1891, 2012.

[4] W. Xie, X. Wang, F. Wang, W. Xu, R. M. Kennel, D. Gerling, and R. D. Lorenz, "Finite-control-set model predictive torque control with a deadbeat solution for pmsm drives," *IEEE Transactions on Industrial Electronics*, vol. 62, no. 9, pp. 5402–5410, 2015.

[5] B. Adhavan, A. Kuppuswamy, G. Jayabaskaran, and V. Jagannathan, "Field oriented control of permanent magnet synchronous motor (pmsm) using fuzzy logic controller," in *2011 IEEE Recent Advances in Intelligent Computational Systems*. IEEE, 2011, pp. 587–592.

[6] L. Dongliang and Z. Lixin, "Application of backstepping control in pmsm servo system," in *2009 9th International Conference on Electronic Measurement & Instruments*. IEEE, 2009, pp. 3–638.

[7] P. Szczupak, "Rapid prototyping system for control of inverters and electrical drives," Ph.D. dissertation, Elektrotechnik, Informationstechnik und Medientechnik, Bergischen Universität Wuppertal, Wuppertal,Deu, 2008.

[8] J. H. Lee and B. Cooley, "Recent advances in model predictive control and other related areas," in *AIChE Symposium Series*, vol. 93, no. 316. New York, NY: American Institute of Chemical Engineers, 1971-c2002., 1997, pp. 201–216.

[9] S. J. Qin and T. A. Badgwell, "An overview of industrial model predictive control technology," in *AIche symposium series*, vol. 93, no. 316. New York, NY: American Institute of Chemical Engineers, 1971-c2002., 1997, pp. 232–256.

[10] P. Cortés, M. P. Kazmierkowski, R. M. Kennel, D. E. Quevedo, and J. Rodríguez, "Predictive control in power electronics and drives," *IEEE Transactions on industrial electronics*, vol. 55, no. 12, pp. 4312–4324, 2008.

[11] J. Rodriguez, M. P. Kazmierkowski, J. R. Espinoza, P. Zanchetta, H. Abu-Rub, H. A. Young, and C. A. Rojas, "State of the art of finite control set model predictive control in power electronics," *IEEE Transactions on Industrial Informatics*, vol. 9, no. 2, pp. 1003–1016, 2012.

[12] K. Belda and D. Vošmik, "Explicit generalized predictive control of speed and position of pmsm drives," *IEEE Transactions on Industrial Electronics*, vol. 63, no. 6, pp. 3889–3896, 2016.

[13] Y. Zhou, H. Li, R. Liu, and J. Mao, "Continuous voltage vector model-free predictive current control of surface mounted permanent magnet synchronous motor," *IEEE Transactions on Energy Conversion*, vol. 34, no. 2, pp. 899–908, 2018.

[14] A. A. Ahmed, B. K. Koh, and Y. I. Lee, "A comparison of finite control set and continuous control set model predictive control schemes for speed control of induction motors," *IEEE Transactions on Industrial Informatics*, vol. 14, no. 4, pp. 1334–1346, 2017.

[15] R. Guzman, L. G. de Vicuña, A. Camacho, J. Miret, and J. M. Rey, "Receding-horizon model-predictive control for a three-phase vsi with an lcl filter," *IEEE Transactions on Industrial Electronics*, vol. 66, no. 9, pp. 6671–6680, 2018.

[16] B. Stellato, T. Geyer, and P. J. Goulart, "High-speed finite control set model predictive control for power electronics," *IEEE Transactions on power electronics*, vol. 32, no. 5, pp. 4007–4020, 2016.

[17] P. Karamanakos, T. Geyer, and R. Kennel, "Reformulation of the long-horizon direct model predictive control problem to reduce the computational effort," in *2014 IEEE Energy Conversion Congress and Exposition (ECCE)*. IEEE, 2014, pp. 3512–3519.

[18] L. Wang, "Use of exponential data weighting in model predictive control design," in *Proceedings of the 40th IEEE Conference on Decision and Control (Cat. No. 01CH37228)*, vol. 5. IEEE, 2001, pp. 4857–4862.

[19] L. M. Grzesiak and T. Tarczewski, "Pmsm servo-drive control system with a state feedback and a load torque feedforward compensation," *COMPEL-The international journal for computation and mathematics in electrical and electronic engineering*, 2013.

[20] L. Wang, *Model predictive control system design and implementation using MATLAB®*. Springer Science & Business Media, 2009.

[21] L. L. Wang, "Discrete model predictive controller design using laguerre functions," *Journal of Process Control*, vol. 14, no. 2, pp. 131–142, 2004.

[22] B. Zhang, C. Zong, G. Chen, and B. Zhang, "Electrical vehicle path tracking based model predictive control with a laguerre function and exponential weight," *IEEE Access*, vol. 7, pp. 17 082–17 097, 2019.

[23] A. Iusem and A. De Pierro, "On the convergence properties of hildreth's quadratic programming algorithm," *Mathematical Programming*, vol. 47, pp. 37–51, 1990.

[24] J. M. Beltran, O. S. Hernandez, R. M. Caporal, P. Ordaz-Oliver, and C. Cuvas-Castillo, "Model predictive torque control of an induction motor with discrete space vector modulation," in *2020 17th International Conference on Electrical Engineering, Computing Science and Automatic Control (CCE)*. IEEE, 2020, pp. 1–6.